Eur. Phys. J. A **36**, 131–138 (2008)
DOI 10.1140/epja/i2008-10587-4

THE EUROPEAN PHYSICAL JOURNAL A

Regular Article – Experimental Physics

Evidence for an isomeric $3/2^-$ state in ^{53}Co

D. Rudolph[1,a], R. Hoischen[1,2], M. Hellström[1], S. Pietri[3], Zs. Podolyák[3], P.H. Regan[3], A.B. Garnsworthy[3,4], S.J. Steer[3], F. Becker[2,b], P. Bednarczyk[2,5], L. Cáceres[2,6], P. Doornenbal[2,7,c], J. Gerl[2], M. Górska[2], J. Grębosz[5,2], I. Kojouharov[2], N. Kurz[2], W. Prokopowicz[2,5], H. Schaffner[2], H.J. Wollersheim[2], L.-L. Andersson[1], L. Atanasova[8], D.L. Balabanski[8,9], M.A. Bentley[10], A. Blazhev[7], C. Brandau[2,3], J.R. Brown[10], C. Fahlander[1], E.K. Johansson[1], and A. Jungclaus[6]

[1] Department of Physics, Lund University, S-221 00 Lund, Sweden
[2] Gesellschaft für Schwerionenforschung mbH, D-64291 Darmstadt, Germany
[3] Department of Physics, University of Surrey, Guildford, GU2 7XH, United Kingdom
[4] Wright Nuclear Structure Laboratory, Yale University, New Haven, CT 06520-8124, USA
[5] The Henryk Niewodniczański Institute of Nuclear Physics (IFJ PAN), PL-31342 Kraków, Poland
[6] Departamento de Física Teórica, Universidad Autónoma de Madrid, E-28049 Madrid, Spain
[7] Institut für Kernphysik, Universität zu Köln, D-50937 Köln, Germany
[8] Faculty of Physics, University of Sofia, BG-1164 Sofia, Bulgaria
[9] Institute for Nuclear Research and Nuclear Energy, Bulgarian Academy of Sciences, BG-1784 Sofia, Bulgaria
[10] Department of Physics, University of York, York, YO10 5DD, UK

Received: 4 March 2008 / Revised: 28 April 2008
Published online: 21 May 2008 –
Communicated by R. Krücken

Abstract. The fragmentation of a 550 MeV/u primary beam of ^{58}Ni on a ^{9}Be target has been used to measure time- and energy-correlated γ decays following the implantation of event-by-event discriminated secondary fragments into a ^{9}Be stopper plate. A new isomeric γ decay with $T_{1/2} = 14(^{6}_{4})$ ns and $E_\gamma = 646.2(2)$ keV is observed and attributed to the decay of the yrast $3/2^-$ state in $^{53}_{27}$Co$_{26}$. This short-lived isomeric state has been populated by means of nuclear reactions during the stopping process of the secondary fragments. The experimental findings are discussed in the framework of large-scale spherical shell model calculations in conjunction with isospin symmetry-breaking residual interactions for the $A = 53$, $T_z = \pm 1/2$ mirror nuclei ^{53}Co and ^{53}Fe.

PACS. 21.60.Cs Shell model – 23.20.-g Electromagnetic transitions – 25.70.Mn Projectile and target fragmentation – 27.40.+z $39 \leq A \leq 58$

1 Introduction

Metastable or isomeric states have a long-standing history in nuclear-structure research [1]. In fact, recent experimental developments have reached a level of detection sensitivity to radiation associated with the decay from such quantum levels which requires the production of less than thousand nuclei of a certain isotope. Thereby, often the first valuable fingerprints become visible for exotic nuclei far from the line of β-stability [2–6].

Of particular interest are isomeric states near doubly magic nuclei, because they efficiently probe the nuclear interaction active at these cornerstones of the spherical shell model —not only by means of precise excitation energies of specific states but more importantly via dynamic and static electromagnetic moments. The situation becomes even more substantial when it is possible to compare and relate the decay characteristics of isobaric analogue states near self-conjugate doubly magic nuclei such as ^{40}Ca or ^{56}Ni. In this mass region, isospin symmetry-breaking effects can be investigated in great detail [7]. This is largely owing to the confinement of the $\mathcal{N} = 3$, "fp shell", combined with the option of reliable large-scale shell model calculations in a spherical harmonic-oscillator basis including well-established residual interactions [8–13].

First steps beyond basic studies of so-called mirror energy differences (MED), which refer to the difference of excitation energies of isobaric analogue states as a function of the angular momentum, have been undertaken. For example, lifetime measurements of specific $I^\pi = 27/2^-$ states in the $A = 51$, $T_z = \pm 1/2$ nuclei $^{51}_{26}$Fe$_{25}$ and $^{51}_{25}$Mn$_{26}$

[a] e-mail: Dirk.Rudolph@nuclear.lu.se
[b] *Present address:* FZ Karlsruhe, D-76344 Eggenstein-Leopoldshafen, Germany.
[c] *Present address:* RIKEN, Saitama 351-0198, Japan.

established on an experimental basis isoscalar and isovector polarization charges near ^{56}Ni by means of absolute and relative $E2$ transition strenghts [14]. These results have recently been confirmed in a study of 10^+ "mirror isomers" in the $T_z = \pm 1$ system $^{54}_{28}\mathrm{Ni}_{26}$ —$^{54}_{26}\mathrm{Fe}_{28}$ [15], while an attempt using the more complex 2^+ states of these two nuclei proved less significant [16].

In the present study we show another test case, namely $3/2^-$ states in the $A = 53$, $T_z = \pm 1/2$ system comprising $^{53}_{27}\mathrm{Co}_{26}$ and $^{53}_{26}\mathrm{Fe}_{27}$ [17]. While the less exotic nuclide ^{53}Fe has been studied rather extensively by light ion transfer and heavy-ion fusion-evaporation reactions [17,18], information on ^{53}Co is rather scarce. The mainly β-decaying $19/2^-$ spin-gap isomer at $E_x = 3190$ keV excitation energy marks the first reported state with a direct proton decay branch [19], but it took more than 30 years for an in-beam γ-ray study to follow. And even so, only the yrast cascade between the $7/2^-$ ground state and an excited $17/2^-$ state at 4.1 MeV could be established. Nevertheless, this allowed for a profound MED study of the $A = 53$, $T_z = \pm 1/2$ mirror pair [20].

The experimental approach is outlined in the next section, followed by a presentation of the experimental results in sect. 3. The shell model calculations and the comparison with the experimental data are the subject of sect. 4.

2 Experimental method

Rare isotopes can be efficiently produced by nuclear fragmentation of a stable heavy-ion beam at relativistic energies on relatively thick targets. Within the *Rare Isotope Spectroscopic INvestigations at GSI* (RISING) campaign [5,6], the nuclei of interest were produced by fragmentation of a ^{58}Ni primary beam at 550 MeV/u on a 1 g/cm^2 Be target. The beam was provided by the UNILAC-SIS accelerator complex at the Gesellschaft für Schwerionenforschung mbH (GSI), Darmstadt, Germany. Due to the high kinetic energy all atomic electrons are fully stripped off the primary beam ions, *i.e.* the charge state $Q = Z = 28$ is being used. The reaction products then enter the approximately 70 m long *FRagment Separator* (FRS) [21] with energies of some 515 MeV/u. A sketch of the FRS and its detector set-up is provided in fig. 1. The fragments, alike the beam particles, start with the charge state $Q = Z$. Because of the relatively low proton number of the fragments in the present case, this maximum charge state is held throughout the passage through the FRS with a probability of essentially 100%.

The fragments pass a first magnetic dipole separation stage of magnetic rigidity $B\rho_1$ and arrive dispersed in momentum at the intermediate focus in an achromatic setting of the FRS. The momentum spread is compensated for by inducing differently matched energy losses, ΔE, in the wedge degrader (cf. fig. 1). In addition, scintillator SC1 provides energy loss signals and position information in the dispersive plane, as well as a timing signal for a time-of-flight measurement for all ions reaching the final focal plane. In the second $B\rho_2$ stage of the FRS the fragments have kinetic energies of 300 to 320 MeV/u, and the

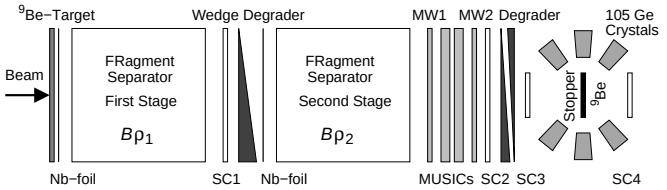

Fig. 1. Schematic drawing of the experimental set-up including the various materials and detectors placed along the beamline. See text and refs. [21,23,24] for details.

typical flight time through the second half of the FRS is approximately 190 ns. Scintillator SC2 provides not only the second signal for the time-of-flight measurement and energy loss and position information, but it also gives the start signal for the RISING Ge-detector array to await prompt and delayed γ radiation coming from those fragments, which are implanted in a 4 mm thick Be plate in the center of the array.

Before finally coming to rest, the fragments i) have passed through multiwire tracking detectors, MW1 and MW2; ii) have given rise to a total of sixteen energy loss signals in two multi-sampling ionisation chambers, MUSIC1 and MUSIC2; iii) have been slowed-down to some 70 MeV/u in an aluminum degrader (to reduce disturbing Bremsstrahlung produced in the stopper); and iv) have been cross-checked for non-destruction via an energy loss measurement in scintillator SC3. The last scintillator SC4 serves as implantation veto.

Invoking the *complete* and thus unequivocal identification scheme of the FRS and its associated detector systems, a total of 8.2 million implanted $A \sim 50$ nuclei have been clearly discriminated by mass, A, and proton number, Z, during about 60 hours of beam time. The implanted beam cocktail comprised ^{51,52}Fe (together 0.4%), ^{52,53}Co (15.5 and 21.3%), and ^{53,54,55}Ni (1.4, 58.6, and 2.8%).

The RISING germanium array itself consists of fifteen high-efficiency CLUSTER germanium detectors [22], providing up front 105 germanium crystals for γ-ray detection, while four crystals were malfunctioning during the experiment. Additionally, on average less than four of the crystals were blinded for delayed nuclear radiation due to the prompt Bremsstrahlung caused by the incoming fragments. The 105 Ge-detector electronics channels were split into two branches, one of which was read out by digital electronics. This branch provided γ-ray energy and γ-ray time in steps of 25 ns with respect to the SC2 trigger signal. The second branch saw a conventional timing sequence of fast signal amplification, constant fraction discrimination, and time-to-digital converters. Here, the timing resolution was down to less than 1 ns per digitized spectrum channel. The data acquisition system was set to wait for about 20 μs after the SC2 trigger signal, then reset itself in waiting position for the next incoming ion. The events were stored in listmode type on computer hard disks, comprising the encoded information of the FRS detectors and time and energy of the correlated, prompt and delayed γ rays. More information on the experiment and the respective RISING set-up can be found in refs. [23–25].

3 Experimental results

The present experimental setting was in principle sensitive only to isomeric states in one of the seven implanted $N < Z$ nuclides mentioned in the previous section and half-lives in the range of $\sim 100\,\mathrm{ns} < T_{1/2} < 50\,\mu\mathrm{s}$. The upper half-life limit was chosen by the experimenters for optimizing the set-up towards the main goal, namely spectroscopy of the 10^+ isomer in ^{54}Ni [15]. The lower limit, however, is an estimate and depends on the number of nuclei produced in the isomeric state of interest with respect to the flight time and, hence, the time period for isomeric decay already *inside* the FRS. Another important quantity, which can reduce the lower limit even further, is the ratio with which the isomer decays by internal conversion —since the fragments are bare nuclei, this decay mode is turned off during the passage through the separator. Good examples for this effect are isomeric states in ^{72}Kr [0_2^+ at 671(2) keV, $T_{1/2} = 26(2)$ ns] [26], ^{74}Kr [0_2^+ at 509(1) keV, $T_{1/2} = 13(7)$ ns] [27,28,26], and ^{200}Pt [7^- and 12^+ states, $T_{1/2} < 15$ ns] [29].

There is yet another possibility for the study of (short-lived) isomeric states, namely via the production by nuclear reactions of the incoming primary fragments along the slowing-down path in the stopper material. For the present experiment this implies a secondary ^{9}Be stopper "target" being subject to mainly ^{52,53}Co and ^{54}Ni secondary beams of some 50 MeV/u down to essentially zero energy, which is reached at some 2–3 mm depth depending on the ion species. Assuming a generic nuclear-reaction cross-section of 1 barn, this gives rise to some

$$8.2 \cdot 10^6 \cdot \frac{0.25\,\mathrm{cm} \cdot 1.85\,\mathrm{g/cm^3}}{9\,\mathrm{g/mol}} \cdot \frac{6 \cdot 10^{23}}{\mathrm{mol}} \cdot 1\,\mathrm{barn} \sim 250000 \quad (1)$$

potential nuclear reactions and, consequently, nuclear-reaction products. Compared with as little as about a thousand implanted ions being necessary for isomeric γ decay detection at RISING (see, *e.g.*, refs. [2,4]), 250000 is clearly a substantial number. However, the observation of such *in situ* populated isomeric states should likely be limited to i) less exotic nuclides (since nuclear-reaction channels with relatively large cross-sections take the nuclear system towards the line of stability), and ii) products close to the incoming fragments, because too violent nuclear processes including the emission of possibly several light particles or fragments could easily trigger the SC4 veto detector and, hence, be disregarded in the offline analysis.

Figure 2 provides three delayed γ-ray spectra correlated with heavy ions implanted in the ^{9}Be stopper. Note the logarithmic scale. The top spectrum and the middle spectrum were taken in the time range from 0.1 μs to 1.0 μs after implantation of ^{54}Ni and combined ^{52,53}Co fragments, respectively. For reference, the bottom spectrum represents the radiation from long-lived background sources. The latter is dominated by the positron annihilation peak at 511 keV, the ^{40}K peak at 1461 keV, and shows several weaker peaks originating from natural thorium and uranium decay chains. In addition, there is one

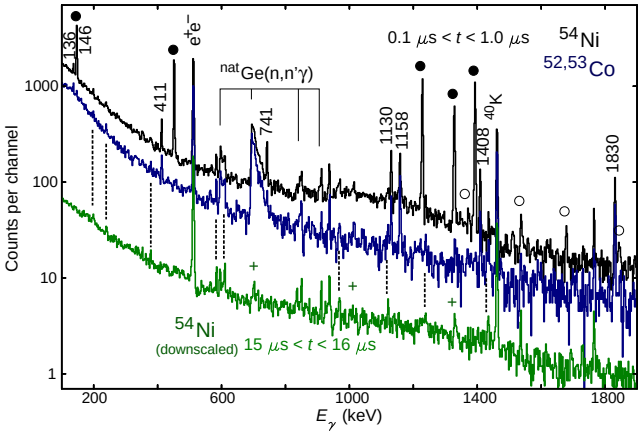

Fig. 2. (Color online) Gamma-ray spectra correlated with implanted ^{54}Ni (top and bottom) and ^{52,53}Co ions (middle). The top and middle spectra were taken between 0.1 and 1.0 μs after implantation, the bottom spectrum between 15 and 16 μs after implantation. The latter is downscaled by a factor of ten for better visibility. Several peaks are marked with their energy in keV, others with their source. Filled circles represent peaks associated with the decay of the 10^+ isomer in ^{54}Ni [15] and open circles denote pile-up of two of the ^{54}Ni transitions in the same or neighbouring Ge crystals. Plus signs label experiment specific long-lived background activity, namely the decay of the $19/2^-$ spin gap isomer in ^{53}Fe [17].

experiment specific long-lived background source, namely the $19/2^-$ spin-gap isomer in ^{53}Fe, which signs responsible for the peaks at 701, 1010, and 1328 keV, marked with "+" in fig. 2. These peaks are also visible in the other two spectra, unless they are covered by lines of different origin with about the same γ-ray energy.

Next to the radiation due to neutron capture reactions in the Ge crystals of the RISING spectrometer, the top spectrum is, of course, dominated by the peaks associated with the decay of the 10^+ isomer in ^{54}Ni [15] —these have energies of 146, 451, 1227, 1327, and 1392 keV, and they are marked with filled circles. The peaks marked with open circles are also related to the ^{54}Ni isomer; they refer to the pile-up of two γ-rays hitting the same or neighbouring Ge crystals, the signals of which were added together if occuring within 50 ns.

Disregarding all peaks in fig. 2 related to (natural) background or the ^{54}Ni isomer, there are several peaks left in *both* the ^{54}Ni *and* the ^{52,53}Co correlated spectrum, namely at 136, (146), 411, 741, 1130, 1158, 1408, and 1830 keV. (Another peak at 3432 keV is out of the range of fig. 2.) Interestingly, all these peaks relate to known isomers in the mass region: the peaks at 136, 1158, and 1830 keV originate from the $19/2^-$ isomer at 3123 keV excitation energy in ^{43}Sc [$T_{1/2} = 470(4)$ ns] [30], the peaks at 146 (doublet with ^{54}Ni), 411, 1130, 1408, and 3432 keV originate from the 10^+ isomer at 6527 keV in ^{54}Fe [$T_{1/2} = 364(7)$ ns] [31], and the peak at 741 keV originates from the $3/2^-$ state at 741 keV in ^{53}Fe [$T_{1/2} = 63.5(14)$ ns] [17]. Note that the three ^{43}Sc related peaks have comparable yields in the two spectra. On the contrary, the peaks

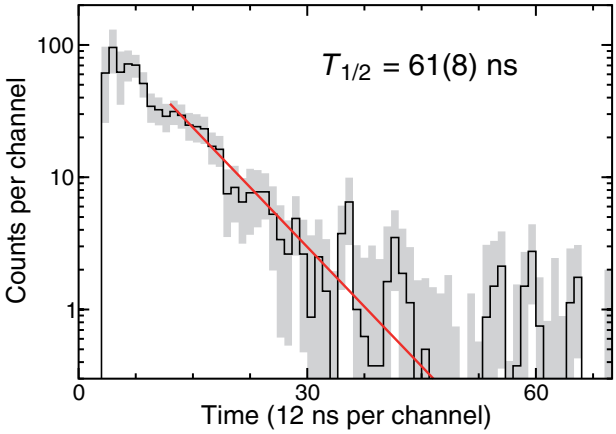

Fig. 3. (Color online) Decay curve of the 741 keV γ-ray (^{53}Fe) following the implantation of ^{54}Ni fragments in the stopper. The data is histogrammed in bins of 12 ns per channel with the grey area providing the experimental uncertainties. The straight line represents a least-squares fit to the data.

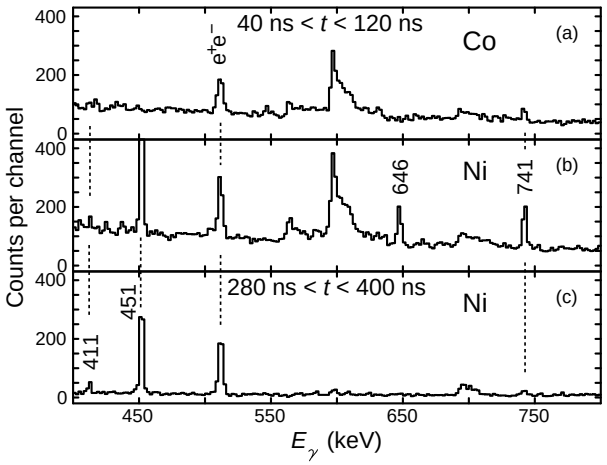

Fig. 4. Gamma-ray spectra correlated with implanted ^{54}Ni (panels (b) and (c)) and ^{52,53}Co ions (panel (a)). The top and middle spectra were taken between 40 and 120 ns after implantation, the bottom spectrum between 280 and 400 ns after implantation. Severeal peaks are marked with their energy in keV. The peak at 511 keV relates to positron annihilation (e^+e^-), and the broad structures between 550 and 630 keV and at about 700 keV are due to radiation from neutron capture reactions in the Ge crystals.

from the ^{54}Fe transitions are somewhat less intense and the ^{53}Fe 741 keV peak is much less intense in the middle, cobalt-correlated spectrum compared with the top, nickel-correlated spectrum. This points towards different nuclear production types in the beryllium stopper for the Sc and Fe isomers, respectively.

The above association of peaks in fig. 2 with isomers in ^{43}Sc and ^{53,54}Fe can, of course, be cross-checked with the time behaviour of the respective decay. As an example, the decay curve of the 741 keV transition is shown in fig. 3. It invokes the conventional RISING time branch (cf. sect. 2), and the data is binned to 12 ns per channel. A least-squares fitting procedure gives $T_{1/2} = 61(8)$ ns for this sample, which is in agreement with the above-mentioned literature value. The peaks suggested to arise from ^{43}Sc and ^{54}Fe can be proven to belong to these two isotopes in a corresponding fashion.

It is also clear that the ^{53}Fe isomer must have been populated in the beryllium stopper, because neither can missing atomic electrons prolong the lifetime, nor can any significant amount of ^{53}Fe produced in the primary target reach the stopper with such a short isomeric half-life —not to mention that the setting of the FRS prohibited transmission of ^{53}Fe (and ^{54}Fe as well as ^{43}Sc) in the first place, and that energy loss correlations in the MUSICs and SC2 and SC3 (cf. fig. 1) ensure implantation of nickel ions.

Figure 4 focuses on short-lived decays by providing γ-ray spectra correlated with ^{52,53}Co (panel (a)) and ^{54}Ni (panels (b) and (c)). While the spectra in figs. 4(a) and (b) were taken between 40 ns and 120 ns after implantation, panel (c) shows a spectrum measured during a somewhat later time window. The broad structures between γ-ray energies of 550 to 630 keV and at about 700 keV again relate to radiation from neutron capture reactions in the Ge crystals. All spectra also reveal once more the positron annihilation peak, and panels (b) and (c) comprise the 451 keV peak from the $6^+ \rightarrow 4^+$ decay in ^{54}Ni. The 411 keV peak from the $6^+ \rightarrow 4^+$ decay in ^{54}Fe becomes more apparent at later times (fig. 4(c)), while the 741 keV $3/2^- \rightarrow 7/2^-$ decay in ^{53}Fe is very pronounced in fig. 4(b), simply because of the earlier time period compared with the top spectrum in fig. 2. Some late remainders of the 741 keV peak are present in fig. 4(c), while it becomes obvious that the $3/2^-$ isomer in ^{53}Fe is produced significantly less efficient with the cobalt ions than with the ^{54}Ni fragments by comparing figs. 4(a) and (b).

Most interestingly, however, there is one additional peak visible at 646 keV in fig. 4(b). It has a similar yield as the 741 keV line, and it is completely absent in both the spectrum correlated with cobalt fragments as well as in the one taken at slightly later times. The latter is an indication for a rather short-lived isomer, while the former observation limits the isotopic origin to either Ni or Co isotopes with $N \sim Z$, *i.e.* most likely to ^{55,56}Ni or ^{53,54,55}Co. Any lighter residue with $Z \leq 26$ would have left a significant signal at 646 keV in fig. 4(a), too. The massive production of exotic $N < Z$ isotopes with $Z \geq 27$ is highly unlikely because of the small reaction cross-sections involved. A data base search [32] for a delayed γ-ray of 646(1) keV in isotopes with $20 \leq N, Z \leq 32$ turned out negative.

^{55}Co has been studied extensively by means of several different experimental approaches [33,34]. So far, no isomeric state has been observed in that nuclide, and due to the shell gap at particle number $N = Z = 28$, excited states in $^{55}_{27}$Co are expected and observed first beyond 2 MeV excitation energy. No signs of the respective ground-state transitions are seen in the present data. Therefore, we exclude ^{55}Co from the list of candidates. Likewise, its mirror nucleus ^{55}Ni is disregarded based on isospin symmetry considerations. The low- to medium-spin regimes of ^{54}Co [31,34,35] and ^{56}Ni [34,36–38] are

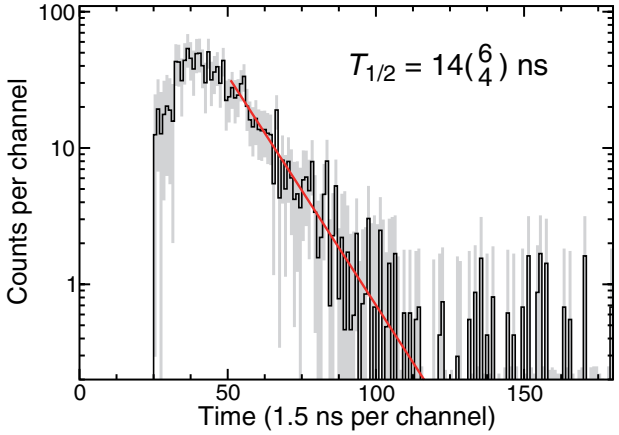

Fig. 5. (Color online) Background-subtracted decay curve of the previously unobserved 646 keV γ-ray following the implantation of ^{54}Ni fragments in the ^{9}Be stopper. The data is histogrammed in bins of 1.5 ns per channel with the grey area providing the experimental uncertainties. The straight line represents a least-squares fit to the data starting some 30 ns after the nominal position of the prompt timing distribution.

also well known, and for reasons similar to the above, also these two nuclei can be disregarded. Thus, the only obvious candidate left is an isomeric state in $^{53}_{27}$Co$_{26}$. Indeed, the mirror nucleus $^{53}_{26}$Fe$_{27}$ does have an isomeric state at comparable excitation energy and half-life, namely the $3/2^-$ state at 741 keV, which is readily observed in figs. 2 and 4, and which has been discussed above.

The decay curve of the 646 keV γ-ray is shown in fig. 5. Due to its short half-life and hence close proximity to the prompt timing peak, the half-life result contains a rather large uncertainty (the least-squares fitting procedure displayed in fig. 5 starts some 30 ns beyond the position of the prompt timing distribution). In conclusion, we attribute the peak at 646.2(2) keV in fig. 4(b) to the decay of an isomeric $I^\pi = 3/2^-$ state in ^{53}Co, situated at 646.2(2) keV excitation energy and with a half-life of $T_{1/2} = 14(^{6}_{4})$ ns. These experimental characteristics are close to the ones of the isobaric analogue state in ^{53}Fe [17].

4 Shell model calculations and discussion

Spherical large-scale shell model calculations were performed with the code ANTOINE [39]. The full fp space is considered including the $1f_{7/2}$ shell below and the $2p_{3/2}$, $1f_{5/2}$, and $2p_{1/2}$ shells above the $N = Z = 28$ shell closure. Nevertheless, the model space has to be truncated allowing a certain number, t, of particles (protons or neutrons) to be excited across the shell closure. Here, a maximum $t = 7$ is chosen to compromise between available computing power and sufficient convergence of the calculated numbers. Both the KB3G [11] and GXPF1A [12, 13] effective interactions have been employed, the predictions of which are generally very reliable for mass $A \sim 50$ nuclei [8–10, 40].

The evolution of the predicted excitation energies of a number of $A = 53$, $T_z = \pm 1/2$ low- to medium-spin

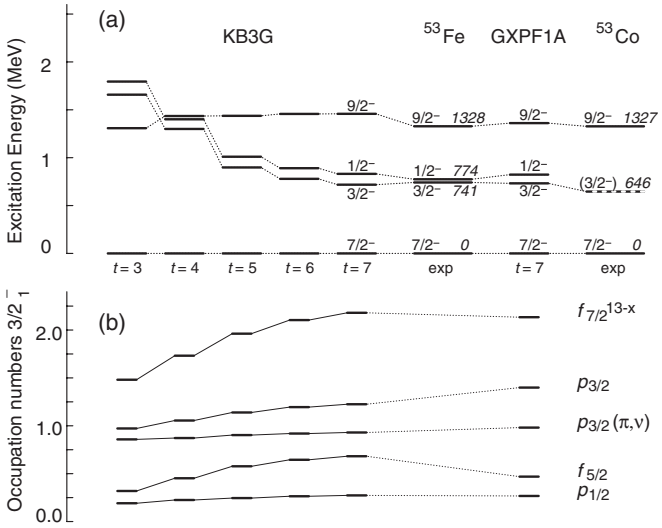

Fig. 6. Results of shell-model calculations for low-spin states in the mass $A = 53$ nuclei ^{53}Co and ^{53}Fe. The left-hand side of panel (a) illustrates the evolution of excitation energies as a function of the number of particles allowed in the upper fp shell, t, for the KB3G [11] fp shell effective interaction. The $t = 7$ predictions using the alternative GXPF1A interaction [13] are included on the right-hand side, surrounded by the respective experimentally known states of the two isobars [17, 20]. Panel (b) illustrates the occupation numbers of the $3/2^-$ yrast state. The plot for the $f_{7/2}$ shell concerns the number of particles *missing* with respect to the originally thirteen particles relative to ^{40}Ca. The plot denoted by $p_{3/2}$ (π, ν) represents the occupation number of only the respective unpaired proton (^{53}Co) or unpaired neutron (^{53}Fe).

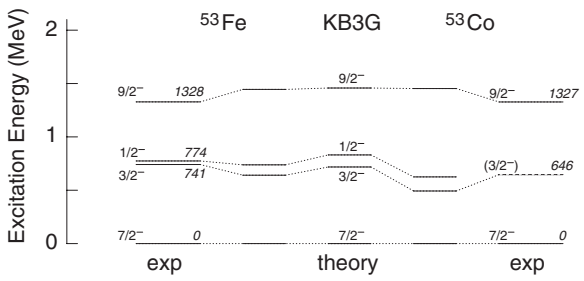

Fig. 7. Comparison of the excitation energies of experimental low-spin states in the mass $A = 53$ nuclei ^{53}Co and ^{53}Fe with predictions from isospin-dependent shell model calculations ($t = 7$) based on the KB3G effective interaction.

states as a function of t is illustrated on the left-hand side of fig. 6(a). An increased t induces in general more correlation energy, but the strongly downsloping excitation energies of the predicted $1/2^-$ and $3/2^-$ low-spin states are apparently much more affected compared with the $9/2^- \rightarrow 7/2^-$ yrast cascade, because the relative energy between these two states remains essentially constant. The $9/2^-$ state, which has been discussed in earlier mass $A = 53$ investigations [18, 20], is included in figs. 6 and 7 as reference.

The enhanced correlations as a function of t find their counterpart in the reduced single-particle character of the

predicted wave functions of the yrast $3/2^-$ ($2p_{3/2}$) state: the $2p_{3/2}$ single-particle partition to the wave function of the $3/2^-$ state drops from 54% ($t = 3$) to 34% ($t = 7$) using KB3G. Figure 6(b) provides the average occupation numbers of the $3/2^-$ state. In line with the above, increasing t increases the average number of proton and neutron holes in the $1f_{7/2}$ shell as well as the average number of protons and neutrons in the $2p_{3/2}$ and $1f_{5/2}$ shells —the latter even more pronounced. The $2p_{1/2}$ shell occupancy does not see any significant change. It is worth mentioning that the occupation number of the unpaired proton (^{53}Co) or unpaired neutron (^{53}Fe), which is denoted $p_{3/2}(\pi, \nu)$ in fig. 6(b), remains essentially constant at about unity. This implies that the correlations are inferred by excitations across the shell gap at $N, Z = 28$ into the $1f_{5/2}$ shell or excitations of the respective other nuclear fluid into the $2p_{3/2}$ shell, *i.e.*, the neutrons in case of ^{53}Co and the protons in case of ^{53}Fe.

Towards the right-hand side of fig. 6 the predictions of a $t = 7$ calculation using the GXPF1A interaction are shown, and in general the results are similar to the predictions based on the KB3G interaction, in particular the calculated energies of the low-spin states. One peculiarity, however, is that the wave function of the yrast $3/2^-$ state predicted by GXPF1A has only about half the $1f_{5/2}$ occupation of the prediction using the KB3G interaction, which is balanced by an on average increased $2p_{3/2}$ occupancy and a slightly reduced number of holes in the $1f_{7/2}$ shell. Moreover, the predicted excitation energy of the yrare $3/2^-_2$ state ($E_x = 1852\,\mathrm{keV}$) differs significantly from the $t = 7$ prediction of the KB3G interaction ($E_x = 2446\,\mathrm{keV}$), while the experimentally known state in ^{53}Fe is situated roughly in between ($E_x = 2043\,\mathrm{keV}$). Such details appear interesting, but they are difficult to trace back to individual two-body matrix-elements or the slightly different single-particle energies of the two effective interactions. Hence, a more thorough theoretical investigation is required.

To study the mirror symmetry of isobaric analogue states in ^{53}Fe and ^{53}Co in more detail, isospin-breaking terms have been incorporated along the notations of refs. [7,9,10]. Multipole harmonic-oscillator Coulomb matrix elements, V_{CM}, the monopole electromagnetic spin-orbit interaction, V_{Cls}, and monopole radial effects have been added to both the bare GXPF1A and KB3G interactions following the prescription of ref. [10]. The matrix element of the effective interaction for two protons in the $1f_{7/2}$ orbital coupled to $J = 2$ has been increased by 100 keV. This isospin-breaking term, usually denoted V_{BM}, has been deduced by Zuker *et al.* [7] from the MED in mass $A = 42$. It showed to be essential to successfully reproduce the MED of several mirror pairs in the mass region [7,9,15,20,41]. To describe the electromagnetic decay properties, effective charges of $e_{eff,p} = 1.15$ and $e_{eff,n} = 0.80$ taken from ref. [14] are used and related to predictions with the standard plain isoscalar values $e_{eff,p} = 1.5$ and $e_{eff,n} = 0.5$ [8]. Magnetic properties are described with free gyromagnetic factors.

Table 1. Mirror energy differences, $E_x(^{53}\mathrm{Co}) - E_x(^{53}\mathrm{Fe})$, for the excited yrast $3/2^-$ and $9/2^-$ states. The calculated numbers are based on the given interactions but involve isospin-breaking components. See text for details.

	Level, I^π	$3/2^-$	$9/2^-$
Experiment	present [20]	−95 keV	−1 keV
Theory	KB3G [11]	−147 keV	8 keV
	GXPF1A [13]	−130 keV	1 keV

The results of the isospin-dependent $t = 7$ calculations based on the KB3G interaction are illustrated in fig. 7. Tables 1 and 2 provide a summary for both the KB3G and GXPF1A interactions. The left-hand side of fig. 7 depicts the comparison of observed and predicted energy levels for ^{53}Fe, while the right-hand side shows the results for ^{53}Co. For reference, the results based on the bare interaction (cf. fig. 6) are repeated in the central part of the figure.

In the case of the yrast $9/2^-$ state the net effect of including isospin-breaking components in the interaction is close to zero; the predicted excitation energies change very little, and the related MED values, *i.e.*, $E_x(^{53}\mathrm{Co}) - E_x(^{53}\mathrm{Fe})$, are small and in nearly perfect agreement with experiment and in line with the discussions in ref. [20]. The actual numbers are summarized in the rightmost column of table 1, and the fact that the MED are small points towards a similar overall structure of the $7/2^-$ ground state and the excited $9/2^-$ state. A closer look at the calculated wave functions of these two states reveals that on average about the same number of protons and neutrons are predicted to be excited across the shell gap for both $A = 53$ nuclei.

The situation is at variance for the $3/2^-$ low-spin yrast state. Here, the wave functions are predicted to comprise distinctively different amounts of protons and neutrons in the $\ell = 1$ p-orbits of the upper fp shell (cf. fig. 6(b)). These protons are less bound and thus easier to excite, and the related energy differences of these excitations lead to large negative MED values for in particular the $3/2^-$ states. The large negative MED prediction is in good agreement with the rather large experimental MED = −95 keV for the $3/2^-$ yrast states. However, including the isospin-breaking components in the shell model calculations, the agreement between experiment and theory on the absolute excitation energy scale is worsened for the presumed single-particle–like $3/2^-$ yrast states (cf. fig. 7). For example, the predicted energy of the $3/2^-$ yrast state for the isospin-symmetric calculation, $E_x = 718\,\mathrm{keV}$ is in line with both the $3/2^-$ state in ^{53}Fe ($E_x = 741\,\mathrm{keV}$, $\Delta E = |E_{x,th} - E_{x,exp}| = 23\,\mathrm{keV}$) and ^{53}Co ($E_x = 646\,\mathrm{keV}$, $\Delta E = 72\,\mathrm{keV}$). However, including the isospin-breaking terms as described above, the predicted excitation energies drop to $E_x = 640\,\mathrm{keV}$ ($\Delta E = 101\,\mathrm{keV}$) for ^{53}Fe and $E_x = 493\,\mathrm{keV}$ for ^{53}Co ($\Delta E = 153\,\mathrm{keV}$), respectively.

The predicted and measured half-lives of some observed low- to medium-spin states in the $A = 53$ nuclei are summarized in table 2. A very good quantitative agreement is achieved for the $11/2^- \to 9/2^- \to 7/2^-$ yrast cascades, and the half-life predictions turn out to be rather

Table 2. Experimental half-lives of experimentally observed states compared to predictions from isospin-dependent fp shell model calculations and using the experimental transition energies for the $A = 53$, $T_z = \pm 1/2$ mirror pair.

	^{53}Fe					^{53}Co				
	Exp [17]	KB3G		GXPF1A		Exp	KB3G		GXPF1A	
State		C1[a]	C2[b]	C1	C2		C1	C2	C1	C2
$1/2^-$	2.0(2) ns	1.8 ns	1.8 ns	4.3 ns	4.3 ns					
$3/2^-$	63.5(14) ns	7.8 ns	13 ns	11 ns	25 ns	$14(^{6}_{4})$ ns	7.6 ns	5.1 ns	7.9 ns	5.0 ns
$5/2^-$	2.8(7) ps	6.0 ps	6.1 ps	4.7 ps	4.8 ps					
$7/2^-_2$	$1.4(^{21}_{7})$	1.6 ps	1.6 ps	1.7 ps	1.6 ps					
$9/2^-$	17(7) fs	24 fs	23 fs	28 fs	27 fs		22 fs	23 fs	25 fs	25 fs
$11/2^-$	53(12) fs	29 fs	28 fs	40 fs	39 fs		27 fs	27 fs	30 fs	31 fs

[a] C1 uses effective charges of $e_{eff,p} = 1.15$ and $e_{eff,n} = 0.80$ [14].
[b] C2 uses effective charges of $e_{eff,p} = 1.5$ and $e_{eff,n} = 0.5$ [8].

independent of the effective charges and effective interaction used. For the yrast $1/2^-$ and $5/2^-$ as well as the yrare $7/2^-_2$ states in ^{53}Fe the agreement is still good.

The crux, however, lies in the predicted half-lives of the yrast $3/2^-$ states. Despite their presumed simplicity of being dominated by $2p_{3/2}$ single-particle components, their half-lives are predicted a factor of 3–8 (^{53}Fe) and 2–3 (^{53}Co) too *short*, *i.e.*, the calculated transition rates are too *fast*. Typically, transition rates are calculated too low because of the lack of the correlations across shell gaps, but in the present case the opposite holds true. Therefore, going to larger values of $t > 7$ or a full fp calculation will not solve the problem. Moreover, the predictions using the effective charges of ref. [14] are worse than the ones neglecting isovector contributions, at variance to other mirror systems in the mass region. This discrepancy becomes most apparent when looking at the comparison of the ratio of the experimental half-lives, which ranges from $R[T_{1/2}(^{53}\mathrm{Fe})/T_{1/2}(^{53}\mathrm{Co})] \sim 3.1$–$6.5$, to the ratio of predicted half-lives, which is close to unity for the calculations with $e_{eff,p} = 1.15$ and $e_{eff,n} = 0.80$. It is only the calculation using the GXPF1A interaction and plain isoscalar effective charges, for which the ratio $R = 5.0$ falls into the experimental ballpark —nevertheless, it is off by almost a factor of three on the absolute scale for both mirror partners. Therefore, a local adjustment of effective charges does not seem to solve the puzzle either, and the answer is considered to rather lie in the nature of the predicted wave functions.

For example, both proton and neutron single-particle energies may be lowered to potentially achieve purer $3/2^-$ states, or a detailed modification of the interaction may be necessary on some decisive two-body matrix elements. While this is considered a purely theoretical prescription beyond the scope of the present work, it should be pointed out that this discrepancy of the decay properties of *both* $3/2^-$ yrast states in the $A = 53$, $T_z = \pm 1/2$ mirror pair is highly unusual considering the overall excellent agreement of large-scale shell model calculations achieved in this mass regime —with or without invoking isospin-breaking terms.

5 Summary

To summarize, short-lived isomeric states have been observed following secondary nuclear reactions of neutron-deficient radioactive $A \sim 50$ fragment beams in a ^{9}Be stopper plate positioned inside the RISING γ-ray spectrometer. A previously unreported delayed γ-ray of 646.2(2) keV with an associated half-life of $T_{1/2} = 14(^{6}_{4})$ ns was observed and attributed to the decay of the $3/2^-$ yrast state of ^{53}Co. Isospin-dependent large-scale shell model calculations agree well with the relative energies of the reported and new isobaric analogue states of the $A = 53$, $T_z = \pm 1/2$ mirror pair. While this type of predictions is commonly in excellent agreement with experimental observations in the upper half of the $1f_{7/2}$ shell, both the calculated absolute energies and, more importantly, the decay strengths of the yrast $3/2^-$ states in ^{53}Co *and* ^{53}Fe deviate considerably from the experimental values. Given the presumed simplicity of this state, this comes as a surprise. On the theoretical side, this calls for a more detailed tracing of the residual interactions and single-particle energies, while experiment may aim at a better definition of the $3/2^-$ states in both the $A = 53$ and $A = 55$ mirror pairs.

The authors gratefully acknowledge the outstanding work of the GSI accelerator and ion source crews in providing the experiment with the envisaged high beam intensities. DR would also like to thank F. Nowacki and G. Kalus for patient support with the new ANTOINE installation. This work is supported by the European Commission contract no. 506065 (EURONS), the Swedish Research Council, EPSRC (UK), the German BMBF under grant 06KY205I, the Polish Ministry of Science and Higher Education under grant 1-P03B-030-30 the Bulgarian Science Fund, grant No. VUF06/05, the Spanish Ministerio de Educación y Ciencia (FPA2005-00696), and the U.S. Department of Energy grants DE-FG02-91ER-40609 and W-31-109-ENG-38.

References

1. P. Walker, G. Dracoulis, Nature **399**, 35 (1999).
2. A. Jungclaus *et al.*, Phys. Rev. Lett. **99**, 132501 (2007).

3. C. Chandler *et al.*, Phys. Rev. C **61**, 044309 (2000).
4. A.B. Garnsworthy *et al.*, Phys. Lett. B **660**, 32 (2008).
5. P.H. Regan *et al.*, Nucl. Phys. A **787**, 491c (2007).
6. D. Rudolph *et al.*, Eur. Phys. J. ST **150**, 173 (2007).
7. A.P. Zuker, S.M. Lenzi, G. Martinez-Pinedo, A. Poves, Phys. Rev. Lett. **89**, 142502 (2002).
8. E. Caurier, G. Martinez-Pinedo, F. Nowacki, A. Poves, A.P. Zuker, Rev. Mod. Phys. **77**, 427 (2005).
9. M.A. Bentley, S.M. Lenzi, Prog. Part. Nucl. Phys. **59**, 497 (2007).
10. J. Ekman, C. Fahlander, D. Rudolph, Mod. Phys. Lett. A **20**, 2977 (2005).
11. A. Poves, J. Sanchez-Solano, E. Caurier, F. Nowacki, Nucl. Phys. A **694**, 157 (2001).
12. M. Honma, B.A. Brown, T. Mizusaki, T. Otsuka, Phys. Rev. C **65**, 061301(R) (2002).
13. M. Honma, B.A. Brown, T. Mizusaki, T. Otsuka, Phys. Rev. C **69**, 034335 (2004); Eur. Phys. J. A **25**, s01, 499 (2005).
14. R. du Rietz *et al.*, Phys. Rev. Lett. **93**, 222501 (2004).
15. D. Rudolph *et al.*, submitted to Phys. Rev. Lett.
16. K.L. Yurkewicz *et al.*, Phys. Rev. C **70**, 054319 (2004).
17. H. Junde, Nucl. Data Sheets **87**, 507 (1999).
18. R. du Rietz *et al.*, Phys. Rev. C **72**, 014307 (2005).
19. K.P. Jackson, C.U. Cardinal, H.C. Evans, N.A. Jelley, J. Cerny, Phys. Lett. B **33**, 281 (1970); J. Cerny, J.E. Esterl, R.A. Gough, R.G. Sextro, Phys. Lett. B **33**, 284 (1970).
20. S.J. Williams *et al.*, Phys. Rev. C **68**, 011301(R) (2003).
21. H. Geissel *et al.*, Nucl. Instrum. Methods B **70**, 286 (1992).
22. J. Eberth, H.G. Thomas, P. von Brentano, R.M. Lieder, H.M. Jäger, H. Kämmerling, M. Berst, D. Gutknecht, R. Henck, Nucl. Instrum. Methods A **369**, 135 (1996).
23. R. Hoischen, Master thesis, Lund University, unpublished, `http://wwwnsg.nuclear.lu.se/projects.asp`.
24. S. Pietri *et al.*, Acta Phys. Pol. **38**, 1255 (2007).
25. S. Pietri *et al.*, Nucl. Instrum. Methods B **261**, 1079 (2007).
26. E. Bouchez *et al.*, Phys. Rev. Lett. **90**, 082502 (2003).
27. C. Chandler *et al.*, Phys. Rev. C **56**, R2924 (1997).
28. F. Becker *et al.*, Eur. Phys. J. A **4**, 103 (1999).
29. M. Caamaño *et al.*, Eur. Phys. J. A **23**, 201 (2005).
30. J.A. Cameron, B. Singh, Nucl. Data Sheets **92**, 783 (2001).
31. H. Junde, H. Su, Nucl. Data Sheets **107**, 1393 (2006).
32. Nuclear Structure and Decay Data base, NuDat 2.4, `http://www.nndc.bnl.gov/nudat2`.
33. H. Junde, Nucl. Data Sheets **64**, 723 (1991) and ENSDF updates.
34. D. Rudolph, C. Baktash, M.J. Brinkman, M. Devlin, H.-Q. Jin, D.R. LaFosse, L.L. Riedinger, D.G. Sarantites, C.-H. Yu, Eur. Phys. J. A **4**, 115 (1999).
35. I. Schneider, A.F. Lisetskiy, C. Frießner, R.V. Jolos, N. Pietralla, A. Schmidt, D. Weisshaar, P. von Brentano, Phys. Rev. C **61**, 044312 (2000).
36. E.K. Johansson *et al.*, Eur. Phys. J. A **27**, 157 (2006).
37. N. Pietralla, private communication.
38. H. Junde, Nucl. Data Sheets **86**, 315 (1999).
39. E. Caurier, shell model code ANTOINE, IReS Strasbourg 1989, 2002; E. Caurier, F. Nowacki, Acta Phys. Pol. **30**, 705 (1999).
40. M. Horoi, B.A. Brown, T. Otsuka, M. Honma, T. Mizusaki, Phys. Rev. C **73**, 061305(R) (2006).
41. A. Gadea *et al.*, Phys. Rev. Lett. **97**, 152501 (2006).